# HIGH-RESOLUTION THROUGH-WALL GHOST IMAGING ALGORITHM USING CHAOTIC MODULATED SIGNAL

*Xiaopeng Wang, Zihuai Lin*

School of Electrical and Information Engineering, The University of Sydney
Email: {xiaopeng.wang, zihuai.lin }@sydney.edu.au

**ABSTRACT**

In this paper, a novel high-resolution through-wall ghost imaging (TWGI) algorithm is proposed for detecting targets hidden behind walls. By using chaotic modulated signals, ghost imaging (GI) derived from optical image reconstruction applications is introduced and applied in through-wall imaging (TWI) scenarios to achieve high-resolution imaging capability. The scattering coefficients of the target imaging plane are treated as levels of brightness in the proposed algorithm, whose spatial distribution can be retrieved by processing the estimated electromagnetic (EM) field at the target imaging plane with the reflected signal captured by a single receiving antenna. Simulation results are presented to show the effectiveness and high quality of reconstruction results by using the proposed TWGI algorithm.

***Index Terms—*** Ghost imaging, Through-wall imaging, Chaotic signal

## 1. INTRODUCTION

In recent decades, the world has been suffering more and more safety issues from terrorist and homeland security threats. As urban environment, which mainly contains indoor and complex obstacle scenario, is the main battlefield of counter-terrorist operations and potential military conflicts in the future, people are concentrating on developing new through-wall surveillance and human-detection methods for close quarters battle (CQB) usage. The ability of penetrating through building walls has therefore made through-wall imaging (TWI) using microwave signals one of the hottest research topics which draws the interest of researchers all over the world. Besides the above military usage, TWI also has a wide range of civilian applications such as fire rescue, emergency relief and disaster survivor searching tasks [1–5].

Although previous TWI algorithms successfully obtain detection results of objects hidden behind walls, the resolution capability is still not satisfied enough, which makes it difficult for operators to classify the weapons or identify hostages from terrorists. Obviously, this is not ideal for practical cases that requires details of the through-wall targets to help providing fast situation awareness and tactical advice.

Ghost imaging (GI) is a high resolution and nonlocal imaging algorithm in the quantum and optical area. The first GI experiment was completed by using two entangled photons under laboratory environment [6] in 1995, followed by the theoretical proof [7] and implementation [8] using classical thermal light in 2004. The principle of GI using classical thermal light is that under the illumination of fully spatial incoherent source, the object can be imaged by calculating the mutual correlation between the reference light field collected by a charge-coupled device (CCD) and the signal received by single bucket pixel detector. This, meanwhile, requires a huge number of measurements [7–9]. Later, the authors in [9] proposed a new imaging reconstruction algorithm which can successfully reduce at least 10 times of the measurements to achieve high resolution results.

In this paper, we propose a novel high resolution TWGI algorithm, in which we exploit the traditional GI algorithm in the field of optics and adapt it into through-wall imaging applications using microwave. With an antenna array radiating chaotic modulated signals, a spatial incoherent electromagnetic (EM) field is generated at the target plane to perform the proposed TWGI. Subsequently, by knowing the dielectric permittivity and thickness of the wall, the EM field at the target imaging plane behind the wall is estimated. The estimated EM field, together with the reflected signal captured by a single receiving antenna, are then processed for the through-wall target image reconstruction.

To our best knowledge, this is the first time to apply the traditional GI algorithm in the field of optics into the area of TWI using microwaves. The proposed algorithm not only improves the resolution of the reconstructed image of the target behind the wall, but also reduces the influence caused by the attenuation of the wall. The imaging effectiveness and reconstruction quality of the proposed algorithm are validated by simulations using both MATLAB and XFDTD.

The organization of the rest of the paper is as follows. In Section 2, fundamental feasibility is discussed, followed by the typical scenario displayed in Section 3. In Section 4, the proposed high-resolution TWGI algorithm is presented. Simulation results are provided in Section 5 to show the effectiveness and the performance of the proposed TWGI. Finally, in Section 6, some conclusions are drawn.

## 2. DERIVATION OF FEASIBILITY

In this Section, we develop the through-wall ghost imaging (TWGI) algorithm using microwave. Two essential points are discussed here, 1) the condition of performing GI using microwave signals and 2) the possibility of successful hidden target image reconstruction using TWGI.

### 2.1. Condition of performing microwave GI

To perform a thermal light ghost imaging, fluctuating light source should be fully spatially incoherent. In traditional thermal light GI scheme, the second order correlation function can be expressed as

$$G^{(1,1)}(x_1, x_2) = I(x_1)\delta(x_1 - x_2) \tag{1}$$

where, $I(x)$ is the intensity distribution of the source and $\delta(x)$ is the Dirac delta function [7]. Obviously, equation (1) indicates that

978-1-4673-6997-8/15/$31.00 ©2015 IEEE

the relationship between different radiation elements on the thermal light source should be statistically independent.

Inspired by the fact that light belongs to electromagnetic wave in essence, it is natural to think about replacing thermal light source with microwave source whose intensity distribution is also expected to satisfy equation (1). Take amplitude as the fluctuation of a single radiation element on a microwave source, the condition described in equation (1) can be written as,

$$G^{(1,1)}(a_{ij}, a_{ij}^{'}) = Amp(a_{ij})\delta(a_{ij} - a_{ij}^{'}) \tag{2}$$

where $G^{(1,1)}(a_{ij}, a_{ij}^{'})$ is the second order correlation function, $Amp(a_{ij})$ is the amplitude distribution of microwave source and $\delta(a_{ij})$ is the Dirac delta function.

Apparently, if we use an antenna array to represent the above microwave source, the condition for performing microwave GI is that for each sub-antenna, as a single radiation element on the array, should transmit amplitude statistically-independent signals

### 2.2. Possibility of target image reconstruction of TWGI

Another crucial condition for performing GI is that under the illumination of spatially incoherent source, only when the field generated at the imaging plane is spatially incoherent, the correlation functions allow to retrieve information about the object [10]. Therefore, the possibility of whether the GI can still be successfully implemented after detecting signals penetrated through the wall should be analyzed.

Consider the situation that a signal $S(t)$ radiates from a single antenna and penetrates through a uniform wall. After one-way penetration, the signal $S_{x_p}(t)$ at a single point $x_p$ in the free space behind the wall can be expressed as,

$$S_{x_p}(t) = \rho S(t - t_{delay}) \tag{3}$$

where, $\rho$ is the attenuation caused by the uniform wall and $t_{delay}$ is the propagation delay including the signal flying time inside and outside the wall [11].

Note that equation (3) indicates that the wall only introduces attenuation and the time delay into the detecting signal. Since the wall is uniform, the attenuation is homogeneous, therefore no correlation has been introduced by the wall. Consequently, the EM fields generated under the illumination of the whole antenna array remain spatially incoherent after detecting signals penetrated through the wall. Thus, the TWGI can be successfully implemented.

## 3. SYSTEM MODEL

The typical application scenario of our proposed TWGI algorithm is shown in Fig. 1. It consists of an antenna array, a single-layered homogeneous wall, the target and the free space. The antenna array of $M^2$ sub-antennas lining in $M$ rows and $M$ columns is placed in front of the wall. The wall is located in the $XZ$-plane with a known dielectric permittivity $\varepsilon$ and a thickness $d$. The target region to be imaged is located along the positive $Y$-axis behind the wall. The reflected signal is collected by a single receiving antenna, which is then processed using our proposed TWGI algorithm to reconstruct the target imaging plane.

From the description in Section 2, in order to satisfy the condition described in equation (2), signal radiated by each sub-antenna should be amplitude statistically-independent. Noise modulated signals possess high statistical independence property by using random modulated waveforms. However, chaotic modulated signals, much

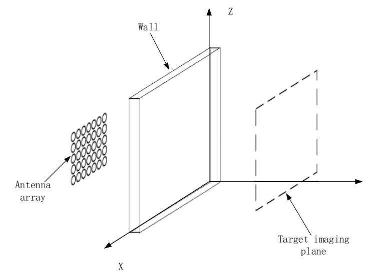


**Fig. 1**. Typical TWI using ghost imaging scenario

like random noise waveforms, not only have the same statistical independence characteristic, their rich dynamical structure and unique deterministic property also offers ease and controllability of generation [12]. Chaos waveforms are generated from dynamical systems, where chaotic maps are one class of the chaotic regimes operating with discrete time steps [12, 13]. In this paper, we formulate cubic mapping to be the nonlinear-dynamic system for generating chaotic amplitude modulated signals to perform our proposed TWGI.

Let $x_{ij}(0)$ be the initial value, the formula of a general term of standard cubic mapping sequence of the signal radiating by one sub-antenna $a_{ij}$ can be expressed as,

$$x_{ij}(n+1) = a(x_{ij}(n))^3 - (1-a)(x_{ij}(n)) \tag{4}$$

where the coefficient $a$ is normally restricted to the range $0 < a \leq 4$ [14].

Then, the chaotic amplitude modulated signal $S_{ij}(t)$ for the sub-antenna $a_{ij}$ can be written as,

$$S_{ij}(t) = Amp_{ij}(t)\exp(2\pi f + \varphi) \tag{5}$$

where

$$Amp_{ij}(t) = \sum_{n} x_{ij}(n) g(t - n\Delta t) \tag{6}$$

In equation (6), g(t) is the standard impulse signal, $\Delta t$ is the discrete sampling interval and $x_{ij}(n)$ is the nth value of the cubic sequence described by equation (4).

## 4. PROPOSED TWGI ALGORITHM

In this section, we first discuss the typical scenario containing a single through-wall point target, then extend to the proposed TWGI algorithm to reconstruct the whole target imaging plane.

### 4.1. Single point target model

Consider a single point target located in a free space hidden behind a uniform wall, under the illumination of the whole antenna array, the reflected signal can be expressed as,

$$r(t) = \rho\delta \sum_{i=1}^{M}\sum_{j=1}^{M} S_{ij}(t - \tau_{ij}) \tag{7}$$

where $\rho$ is the attenuation caused by the wall, $\delta$ is the scattering coefficient of the single point target, $S_{ij}(t)$ is the chaotic modulated signal transmitting by a single sub-antenna on the array and $\tau_{ij}$ is the propagation delay including the signal flying time inside and outside the wall. Given the precise wall thickness and dielectric constant, the traveling distances of the detecting signal inside and outside the wall can be accurately computed. Based on the traveling distances, the propagation delay $\tau_{ij}$ can be calculated [11].

### 4.2. TWGI for the whole imaging plane

If we think the above single point target as a single pixel in the reconstruction target image, then the scattering coefficient $\delta$ can be treated as the brightness level indicating reflectivity at the certain spatial location. To be more specific, the target image can be reconstructed by recovering the spatial distribution of scattering coefficients at the target imaging plane.

Extend the above single target model and divide the whole target imaging plane behind the wall into a finite number of sub-planes with P rows and Q columns. Each sub-plane can be treated as a single point target, whose scattering coefficient represents the corresponding sub-plane. Let the matrix of center locations of the sub-planes to be expressed as,

$$\mathbf{Y}_{P\times Q} = \begin{bmatrix} y_{11} & \cdots & y_{1Q} \\ \vdots & \ddots & \vdots \\ y_{P1} & \cdots & y_{PQ} \end{bmatrix} \tag{8}$$

Then the distribution of scattering coefficients of the imaging plane behind the wall can be expressed as,

$$\mathbf{\Delta}_{P\times Q} = \begin{bmatrix} \delta_{11} & \cdots & \delta_{1Q} \\ \vdots & \ddots & \vdots \\ \delta_{P1} & \cdots & \delta_{PQ} \end{bmatrix} \tag{9}$$

Apparently, the resolution of our proposed TWGI algorithm is governed by the size of sub-planes.

The algorithm proposed in [9] links the relationship between received signals and thermal light fields at the target imaging plane by transmissivity. The image is recovered by solving the spatial distribution of the transmissivity at the imaging plane. Since the transmissivity and scattering coefficients both describe the impulse response of the system containing target imaging plane, the above algorithm can therefore be exploited into TWGI scenario,

$$\begin{bmatrix} R_1 \\ R_2 \\ \vdots \\ R_N \end{bmatrix} = \rho \begin{bmatrix} E_{1,1}^{(1)}, & \ldots E_{p,1}^{(1)}, & \ldots E_{P,Q}^{(1)} \\ E_{1,1}^{(2)}, & \ldots E_{p,1}^{(2)}, & \ldots E_{P,Q}^{(2)} \\ \vdots & \vdots & \vdots \\ E_{1,1}^{(N)}, & \ldots E_{p,1}^{(N)}, & \ldots E_{P,Q}^{(N)} \end{bmatrix} \begin{bmatrix} \delta_{1,1} \\ \delta_{2,1} \\ \vdots \\ \delta_{P,Q} \end{bmatrix} \tag{10}$$

where, $R_n(n = 1, 2, \ldots N, N = P \times Q)$ is the received signal of N times detection, $\rho$ is the attenuation caused by the uniform wall, $E_{p,q}^{(n)}$ is the EM field at one sub-plane $y_{11}$ in the $n$th detection,

$$E_{p,q}^{(n)} = \sum_{i=1}^{M} \sum_{j=1}^{M} S_{ij}(t - \tau_{ij}) \tag{11}$$

Equation(10) can be rewritten as,

$$\mathfrak{R} = \rho \mathfrak{E} \boldsymbol{\delta} \tag{12}$$

then,

$$\boldsymbol{\delta} = \rho \mathfrak{E}^{-1} \mathfrak{R} \tag{13}$$

Equation(13) shows that if the matrix of EM field $\mathfrak{E}$ at the imaging plane is full rank, there will exists a unique solution for the distribution of scattering coefficients at the target imaging plane.

Note that, the attenuation $\rho$ caused by the uniform wall can be treated as a linear scale coefficient in the reconstruction result, in other words, the proposed through-wall imaging algorithm is not sensitive to the attenuation under the condition of the uniform wall.

### 4.3. Sampling adjustment for TWGI

According to the condition discussed in Section 2.2, under the illumination of the whole antenna array, the EM field at the imaging plane behind the wall is spatially incoherent, which can make $\mathfrak{E}$ to be full rank. However, since TWI applications mainly contain close quarter scenarios where the difference in propagation distance from different sub-antennas to the sub-planes could not be ignored, the sampling time points for detection should be adjusted to make the imaging plane to be covered by the illumination of the whole antenna array.

Let $y_{p,q} \in \mathbf{Y}_{P\times Q}$ be the center location of an arbitrary sub-plane, the total propagation time from the whole antenna array to the center location of the sub-plane $y_{p,q}$ is given by,

$$\boldsymbol{T}_{total\_y_{p,q}} = \boldsymbol{T}_{wall\_y_{p,q}} + \boldsymbol{T}_{out\_y_{p,q}} \tag{14}$$

where, $\boldsymbol{T}_{wall\_y_{p,q}}$ and $\boldsymbol{T}_{out\_y_{p,q}}$ is the propagation time matrix from each sub-antenna on the whole antenna array to the sub-plane $y_{p,q}$ inside and outside the wall respectively. Then with equation (11), the reflected signal from $y_{p,q}$ can be rewritten as,

$$r_{p,q}(t) = \rho \delta_{p,q} E_{p,q}(t - \boldsymbol{T}_{total\_y_{p,q}}) \tag{15}$$

here, $\delta_{p,q}$ is the scattering coefficient of the single sub-plane, $\rho$ is the attenuation caused by the uniform wall, and $E_{p,q}(t - \boldsymbol{T}_{total\_y_{p,q}})$ is the EM field at the single sub-plane $y_{p,q}$.

The total propagation time from the antenna array to the whole imaging plane can be expressed as,

$$\mathbf{\Gamma} = \begin{bmatrix} \boldsymbol{T}_{total\_y_{1,1}} & \cdots & \boldsymbol{T}_{total\_y_{1,Q}} \\ \vdots & \ddots & \vdots \\ \boldsymbol{T}_{total\_y_{P,1}} & \cdots & \boldsymbol{T}_{total\_y_{P,Q}} \end{bmatrix} \tag{16}$$

Let $\gamma_{min}$ and $\gamma_{max}$ be the minima and the maxima in $\mathbf{\Gamma}$, respectively. For an arbitrary sub-plane $y_{p,q}$, the adjusted time period for sampling can be expressed as,

$$\boldsymbol{T}_{period\_y_{p,q}} = [(\gamma_{max} - \boldsymbol{T}_{total\_y_{p,q}}), (\gamma_{min} + T_p - \boldsymbol{T}_{total\_y_{p,q}})] \tag{17}$$

where $T_p$ is the width of the detecting signal.

Since the detecting signal is statistically independent, the EM field distribution at an arbitrary time point $t_n \in \boldsymbol{T}_{period\_y_{p,q}}$ is one slice of the state of the EM field generated by the whole antenna array, which is spatially incoherent and can be treated as one detection. Therefore, equation (10) can be rewritten as equation (18),

The target imaging plane behind the wall can then be reconstructed by solving (18) to get the spatial distribution of scattering coefficients.

## 5. SIMULATION RESULTS

In this section, simulation results are presented to demonstrate the effectiveness of our proposed TWGI algorithm. In the following simulations, the target imaging plane is placed at a distance of 4m behind the uniform concrete wall. The dielectric permittivity of the wall is set to be $\varepsilon = 9$ and thickness is $d = 0.1$m. The transmitting

$$\begin{bmatrix} R_{(t_1)} \\ R_{(t_2)} \\ \vdots \\ R_{(t_N)} \end{bmatrix} = \rho \begin{bmatrix} E_{period\_y_{1,1}}(t_1), & \dots & , E_{period\_y_{p,1}}(t_1), & \dots & , E_{period\_y_{P,Q}}(t_1) \\ E_{period\_y_{1,1}}(t_2), & \dots & , E_{period\_y_{p,1}}(t_2), & \dots & , E_{period\_y_{P,Q}}(t_2) \\ \vdots & & \vdots & & \vdots \\ E_{period\_y_{1,1}}(t_n), & \dots & , E_{period\_y_{p,1}}(t_n), & \dots & , E_{period\_y_{P,Q}}(t_n) \end{bmatrix} \begin{bmatrix} \delta_{1,1} \\ \delta_{2,1} \\ \vdots \\ \delta_{P,Q} \end{bmatrix} \tag{18}$$

sub-antennas are placed to form a circular antenna array and a single receiving antenna is placed in the center of the location.

### 5.1. MATLAB Simulation result

We first verify the proposed TWGI algorithm using MATLAB, where target imaging plane behind the wall is divided into $20 \times 20$ sub-planes. The detecting signal is the chaotic amplitude modulated signal with the carrier of sinusoidal wave at the center frequency of 1GHz. Fig.2 (a) and Fig.2 (b) shows the chaotic modulated signal and its self-correlation respectively, indicating that the antenna array performs as a fully incoherent source. Fig 2 (c) shows one slice of the state of the EM field at the target imaging plane under the illumination of the whole antenna array. Fig2 (d) shows that the EM field is spatially incoherent which satisfied the condition discussed in section 2.2. This confirms that the generated field behind the wall can successfully perform the proposed TWGI.

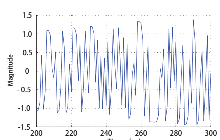

(a) Chaotic Signal

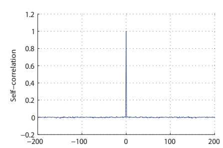

(b) Self-correlation

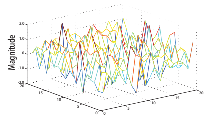

(c) Electromagnetic Field

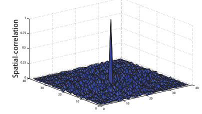

(d) Spatial-correlation

**Fig. 2**. Chaotic Signal and EM Field at Target Imaging Plane.

Compared with the original distribution of scattering coefficients at the through-wall target plane displayed in Fig.3 (a), our proposed TWGI algorithm accurately reconstructs the image with clear edge, which is shown in Fig.3 (b).

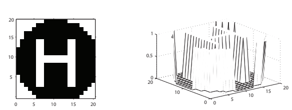
(a) Original Distribution of Scattering Coefficients

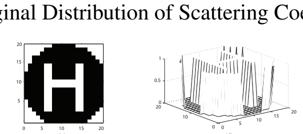
(b) Reconstructed Distribution of Scattering Coefficients

**Fig. 3**. Image Reconstruction Results by MATLAB.

### 5.2. XFDTD Simulation result

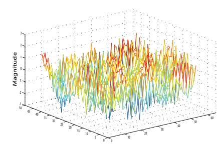
(a) Electromagnetic field

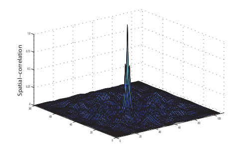
(b) Spatial-correlation

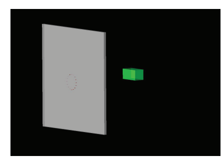
(c) Scenario with cubic box

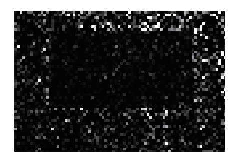
(d) Reconstruction of cubic box

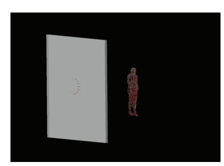
(e) Scenario with human body


(f) Reconstruction of human body

**Fig. 4**. Detecting signal and EM field at target imaging plane.

Besides the simulations by using MATLAB, we also used XFDTD to simulate the scenario. Two target objects are investigated: a cubic box and a human body. Fig.4 (a) and Fig. 4 (b) shows that the EM field generated at the target imaging plane behind the wall possesses high spatial coherent characteristic, which also confirms the possibility of successfully performing the proposed TWGI algorithm.

Fig.4 (c) and (e) displays the geometry settings of the cubic box and human body, and reconstruction results are presented in Fig.4 (d) and (f), respectively. Even with noise points in the picture, this raw reconstruction results show a better performance with clearer edge and less fake images, compared with those presented in the existing literature, e.g., [1] and [2, 3].

## 6. CONCLUSIONS

In this paper, based on the chaotic modulated signal and the ghost imaging (GI) technique traditionally used in the optical area, we proposed a novel high-resolution and attenuation-insensitive TWGI algorithm. Simulation results by using MATLAB and XFDTD showed that the proposed TWGI algorithm provided high quality reconstruction results under the scenario of uniform walls with different through-wall hidden targets.

## 7. REFERENCES


[1] G. Gennarelli, G. Riccio, R. Solimene, and F. Soldovieri, "Radar imaging through a building corner," *Geoscience and Remote Sensing, IEEE Transactions on*, vol. 52, no. 10, pp. 6750–6761, Oct 2014.

[2] Wenji Zhang and A Hoorfar, "Three-dimensional synthetic aperture radar imaging through multilayered walls," *Antennas and Propagation, IEEE Transactions on*, vol. 62, no. 1, pp. 459–462, Jan 2014.

[3] Wenji Zhang and A Hoorfar, "Three-dimensional real-time through-the-wall radar imaging with diffraction tomographic algorithm," *Geoscience and Remote Sensing, IEEE Transactions on*, vol. 51, no. 7, pp. 4155–4163, July 2013.

[4] Wenji Zhang, Qing Huo Liu, and A Hoorfar, "Three-dimensional real-time through-the-wall imaging," in *Antennas and Propagation Society International Symposium (APSURSI), 2012 IEEE*, July 2012, pp. 1–2.

[5] F. Ahmad, Yimin Zhang, and M.G. Amin, "Three-dimensional wideband beamforming for imaging through a single wall," *Geoscience and Remote Sensing Letters, IEEE*, vol. 5, no. 2, pp. 176–179, April 2008.

[6] TB Pittman, YH Shih, DV Strekalov, and AV Sergienko, "Optical imaging by means of two-photon quantum entanglement," *Physical Review A*, vol. 52, no. 5, pp. R3429, 1995.

[7] Jing Cheng and Shensheng Han, "Incoherent coincidence imaging and its applicability in x-ray diffraction," *Physical review letters*, vol. 92, no. 9, pp. 093903, 2004.

[8] Alessandra Gatti, Enrico Brambilla, Morten Bache, and Luigi A Lugiato, "Ghost imaging with thermal light: comparing entanglement and classicalcorrelation," *Physical review letters*, vol. 93, no. 9, pp. 093602, 2004.

[9] Liu Jiying, Zhu Jubo, Lu Chuan, and Huang Shisheng, "High-quality quantum-imaging algorithm and experiment based on compressive sensing," *Optics letters*, vol. 35, no. 8, pp. 1206–1208, 2010.

[10] A Gatti, Morten Bache, D Magatti, E Brambilla, F Ferri, and LA Lugiato, "Coherent imaging with pseudo-thermal incoherent light," *Journal of Modern Optics*, vol. 53, no. 5-6, pp. 739–760, 2006.

[11] Yang Zhao, Biying Lu, and Xin Sun, "Three-dimensional imaging for uwb though-the-wall radar," in *Information Science and Technology (ICIST), 2013 International Conference on*, March 2013, pp. 1503–1506.

[12] V. Venkatasubramanian, H. Leung, and Xiaoxiang Liu, "Chaos uwb radar for through-the-wall imaging," *Image Processing, IEEE Transactions on*, vol. 18, no. 6, pp. 1255–1265, June 2009.

[13] VI Afanas' ev, "Chaotic waveform generator using a turbulent electron beam," in *Physics and Engineering of Millimeter and Sub-Millimeter Waves, 2001. The Fourth International Kharkov Symposium on*. IEEE, 2001, vol. 2, pp. 562–564.

[14] Thomas D Rogers and David C Whitley, "Chaos in the cubic mapping," *Mathematical Modelling*, vol. 4, no. 1, pp. 9–25, 1983.